© 2018. Published by The Company of Biologists Ltd | Development (2018) 145, dev165613. doi:10.1242/dev.165613

HUMAN DEVELOPMENT

RESEARCH ARTICLE

Termination of cell-type specification gene programs by the miR-183 cluster determines the population sizes of low-threshold mechanosensitive neurons

Changgeng Peng[1,‡], Alessandro Furlan[2,*], Ming-Dong Zhang[2,*], Jie Su[2,*], Moritz Lübke[2], Peter Lönnerberg[2], Hind Abdo[2], Jana Sontheimer[2], Erik Sundström[3] and Patrik Ernfors[2,‡]

ABSTRACT

Touch and mechanical sensations require the development of several different kinds of sensory neurons dedicated to respond to certain types of mechanical stimuli. The transcription factor Shox2 (short stature homeobox 2) is involved in the generation of TRKB$^+$ low-threshold mechanoreceptors (LTMRs), but mechanisms terminating this program and allowing alternative fates are unknown. Here, we show that the conditional loss of the miR-183-96-182 cluster in mouse leads to a failure of extinction of Shox2 during development and an increase in the proportion of Aδ LTMRs (TRKB$^+$/NECAB2$^+$) neurons at the expense of Aβ slowly adapting (SA)-LTMRs (TRKC$^+$/Runx3$^-$) neurons. Conversely, overexpression of miR-183 cluster that represses Shox2 expression, or loss of Shox2, both increase the Aβ SA-LTMRs population at the expense of Aδ LTMRs. Our results suggest that the miR-183 cluster determines the timing of Shox2 expression by direct targeting during development, and through this determines the population sizes of Aδ LTMRs and Aβ SA-LTMRs.

KEY WORDS: miR-183-96-182, Shox2, Dorsal root ganglia, Sensory neuron, Specification, Fate switch

INTRODUCTION

Sensory neurons are heterogeneous: some neuron types have a low activation threshold and are therefore highly sensitive to stimuli. These register non-painful low-threshold mechanical stimuli and are therefore termed low-threshold mechanosensitive neurons. Myelinated (A-fiber type) low-threshold mechanoreceptors (LTMRs) terminate peripherally in the skin and participate in touch sensation. Interestingly, based on single-cell RNA sequencing, there are three types of myelinated LTMR: Aδ LTMRs, Aβ rapidly adapting (Aβ RA) LTMRs and Aβ slowly adapting (Aβ SA) LTMRs [referred to as NF1, NF2 and NF3 by Usoskin et al. (2015)]. Aδ LTMRs terminate as longitudinal lanceolate endings in hair follicles, and are involved in directional sensitivity to hair deflection and light touch. Aβ RA-LTMRs terminate as three morphologically distinct types of nerve ending: in Meissner corpuscles in glabrous skin, which detect movement across the skin; in Pacinian corpuscles in glabrous skin, which are tuned to high-frequency vibration; and in lanceolate endings in hairy skin, which detect movement and low-frequency vibration (Abraira and Ginty, 2013). Finally, Aβ SA-LTMRs terminate on Merkel cells in hairy and glabrous skin, and are involved in sensitivity to skin indentation; in addition, when terminating as circumferential endings in hair follicles, they mediate sensitivity to gentle skin stroking. These three types of myelinated LTMR can be defined by: expression of NECAB2 and high levels of TRKB (Aδ LTMRs); expression of CALB1, RET and low levels of TRKB (Aβ RA-LTMRs); and finally, expression of TRKC and RET (Aβ SA-LTMRs) (Usoskin et al., 2015).

During development, touch-sensitive neurons are specified from a common progenitor pool by a series of instructive signals and transcription factors (Lallemend and Ernfors, 2012; Liu and Ma, 2011). Early hybrid TRKB$^+$/TRKC$^+$ neurons diverge around E11-E12 in the mouse and eventually generate two mature TRKB$^+$ (NTRK2$^+$) neuronal types, TRKB^{high} Aδ LTMRs and TRKB^{low} Aβ RA LTMRs, both of which extinguish TRKC (NTRK3) expression, whereas those that maintain TRKC but extinguish TRKB expression become Aβ SA-LTMRs neurons (Bourane et al., 2009; Kramer et al., 2006; Lallemend and Ernfors, 2012). In contrast to the above touch-sensitive neuron types, TRKC$^+$ proprioceptive mechanosensitive neurons express RUNX3, which promotes the proprioceptive neuronal fate (Abdo et al., 2011; Kramer et al., 2006; Levanon et al., 2002; Scott et al., 2011).

MicroRNAs (miRNAs) can play a crucial role during development. For example, one of the first miRNAs identified, Lin-4, regulates developmental timing across different tissues in the nematode *C. elegans*, and loss-of-function mutations reiterate early developmental programs at inappropriate late larval stages (Chalfie et al., 1981; Lee et al., 1993; Wightman et al., 1993). For development of sensory systems, the miR-183-96-182 (the miR-183 cluster) is particularly interesting because it is expressed in many sensory organs, such as retina, inner ear, dorsal root ganglion (DRG), olfactory epithelia and tongue epithelia in mouse (Bak et al., 2008; Lagos-Quintana et al., 2003; Lumayag et al., 2013; Sacheli et al., 2009). A high expression level of the miR-183 cluster in retina is necessary for the development of its outer segments and functional maintenance in the adult (Busskamp et al., 2014a,b; Lumayag et al., 2013; Zhu et al., 2011). The miR-183 cluster also regulates the development of sensory inner ear hair cells, and point mutations on *miR-96* affects hair cell function or hair cell development [causing progressive hearing loss in both mouse and human (Gu et al., 2013; Lewis et al., 2009; Mencía et al., 2009; Soldà et al., 2012)]. In this work, we conditionally delete the miR-183 cluster in neural crest derivatives, including the DRG. We report that the miR-183 cluster is expressed in DRG sensory neuron progenitors where it acts as a timer

[1]The First Rehabilitation Hospital of Shanghai, Tongji University School of Medicine, 200029 Shanghai, China. [2]Department of Medical Biochemistry and Biophysics, Division of Molecular Neurobiology, Karolinska Institutet, 17177 Stockholm, Sweden. [3]Department of Neurobiology, Care Sciences and Society, Karolinska Institutet, 17177 Stockholm, Sweden.
*These authors contributed equally to this work

‡Authors for correspondence (changgeng.peng@tongji.edu.cn; patrik.ernfors@ki.se)

M.L., 0000-0002-8103-0185; P.E., 0000-0002-1140-3986

Received 20 March 2018; Accepted 3 August 2018

Development (2018) 145, dev165613. doi:10.1242/dev.165613

to extinguish *Shox2* through direct targeting of its mRNA, which aborts the gene programs for Aδ NECAB2^{+}TRKB^{high} LTMR neurons and re-directs cell specification towards the generation of Aβ TRKC^{+}RUNX3^{-} SA-LTMR neurons.

RESULTS

Loss of miR-183 cluster shifts the proportions of TRKB and TRKC neurons during embryonic development

All three miR-183 cluster members (*miR-183*, *miR-96* and *miR-182*) are specifically expressed in mouse DRG already at E10.5 and are continuously expressed through development into adulthood (Peng et al., 2017). To directly examine whether the miR-183 cluster plays a role in somatosensory neuron development, we crossed *Wnt1-Cre* mice (Danielian et al., 1998) with *miR-183-96-182*$^{flox/flox}$ mice (Peng et al., 2017) to generate *Wnt1-Cre; miR-183-96-182*$^{flox/flox}$ conditional knockout mice lacking the miR-183 cluster in all DRG neurons (referred to as *miR*^{CKO} mice). *In situ* hybridization confirmed that expression of the miR-183 cluster was depleted in DRG from E11.5 onwards in the *miR*^{CKO} mice (Fig. S1A). Immunohistochemical analysis of newly born (P0) mice revealed that the proportion of TRKB^{+} neurons was increased in the *miR*^{CKO} mice when compared with *Wnt1-Cre* mice (Fig. 1A-C). Importantly, the total number of neurons in L5 DRG was unchanged (Fig. 1D). In contrast, the percentage of TRKC^{+} neurons was decreased in the *miR*^{CKO} mice. This reduction was caused by a decrease in development of TRKC^{+}/RUNX3^{-} sensory neurons (Aβ SA-LTMRs), whereas TRKC^{+}/RUNX3^{+} proprioceptive neurons appear to be unchanged (Fig. 1E-G). Loss of the miR-183 cluster had no effect at P0 on the proportions of TRKA (nociceptors), RET (some nociceptors and some LTMRs), neurofilament heavy polypeptide (NFH, all LTMRs), RET^{+}/NFH^{+} (RET^{+} LTMRs) and RET^{-}/NFH^{+} (all LTMRs except RET^{+}) in the *miR*^{CKO} mice when compared with *Wnt1-Cre* mice (Fig. S1B,C). These data suggest that loss of the miR-183 cluster leads to fate-switch specifically of TRKC^{+} to TRKB^{+} neurons in the DRG without any changes in absolute numbers of LTMRs.

The miR-183 cluster controls the time window of Shox2 expression in DRG neurons

To identify the mechanism by which the miR-183 cluster works to cause change of the fate of early DRG progenitor cells, we profiled RNA expression by RNA sequencing in three biological replicates of E12.5 lumbar DRG from the *miR*^{CKO} and control mice (Table S1, sheet 1). A total of 777 genes were significantly (P<0.05) upregulated in the *miR*^{CKO} DRG when analyzing the RNA sequencing data using Qlucore (Fig. 2A; Table S1, sheet 2). Among these, 101 genes were putative direct targets carrying binding site(s) for at least two members of the miR-183 cluster predicted by TargetScan algorithm (www.targetscan.org; Table S1, sheet 3), and 38 out of the 101 genes were increased with more than 1.3-fold in the absence of the miR-183 cluster (Fig. 2B; Table S1, sheet 4). Only two of these were transcription factors (Shox2 and Zbtb41); however, Shox2 was among the top 10 highly expressed genes with more than 1.3-fold upregulation (Table S1, sheet 4). This caught our attention, because Shox2 has been reported to be important for proper specification of TRKB^{+} neurons in the developing DRG (Abdo et al., 2011; Scott et al., 2011). Furthermore, two highly conserved binding sites for *miR-183* and *miR-96* in the *Shox2* 3′UTR were predicted by TargetScan algorithm among many vertebrates (Fig. S2). Real-time PCR independently confirmed that *Shox2* mRNA was increased 2.3-fold in the *miR*^{CKO} compared with control mice at E12.5 (Fig. 2C). SHOX2 protein was highly expressed in most DRG

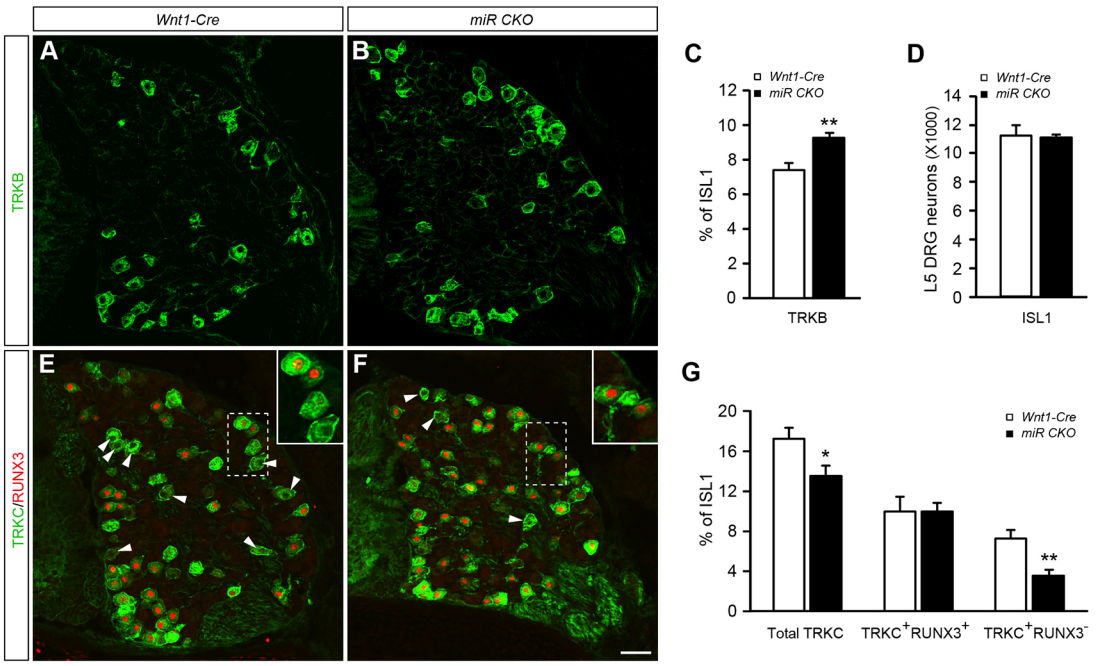

Fig. 1. The population sizes of TRKB^{+} and TRKC^{+} neurons are altered in the P0 *miR*^{CKO} mice. (A-C) The percentage of TRKB^{+} neurons was increased in the *miR*^{CKO} mice. Immunostaining for TRKB on DRG sections of control *Wnt1-Cre* mice (A) and the *miR*^{CKO} mice (B), as well as quantification of the percentage of TRKB^{+} neurons in L3-L5 ganglions (C, n=3 and 4). (D) The number of total neurons (ISL1^{+}) in L5 DRG was not altered in the *miR*^{CKO} mice compared with controls (n=3 and 4; not significant). (E-G) The percentage of TRKC^{+} neurons was decreased in the *miR*^{CKO} mice. Double immunostaining for TRKC and RUNX3 on DRG sections of *Wnt1-Cre* mice (E) and *miR*^{CKO} mice (F). Arrowheads in E and F indicate NF3 (TRKC^{+}RUNX3^{-}) neurons; insets are higher magnifications of areas outlined in E and F. (G) Quantification of the percentage of TRKC^{+}, TRKC^{+}RUNX3^{+} (not significant) and TRKC^{+}RUNX3^{-} neurons in L3-L5 ganglions (n=4). Data are mean±s.e.m. and analyzed by t-test. *P<0.05, **P<0.01. Scale bar: 50 µm.

Development (2018) 145, dev165613. doi:10.1242/dev.165613

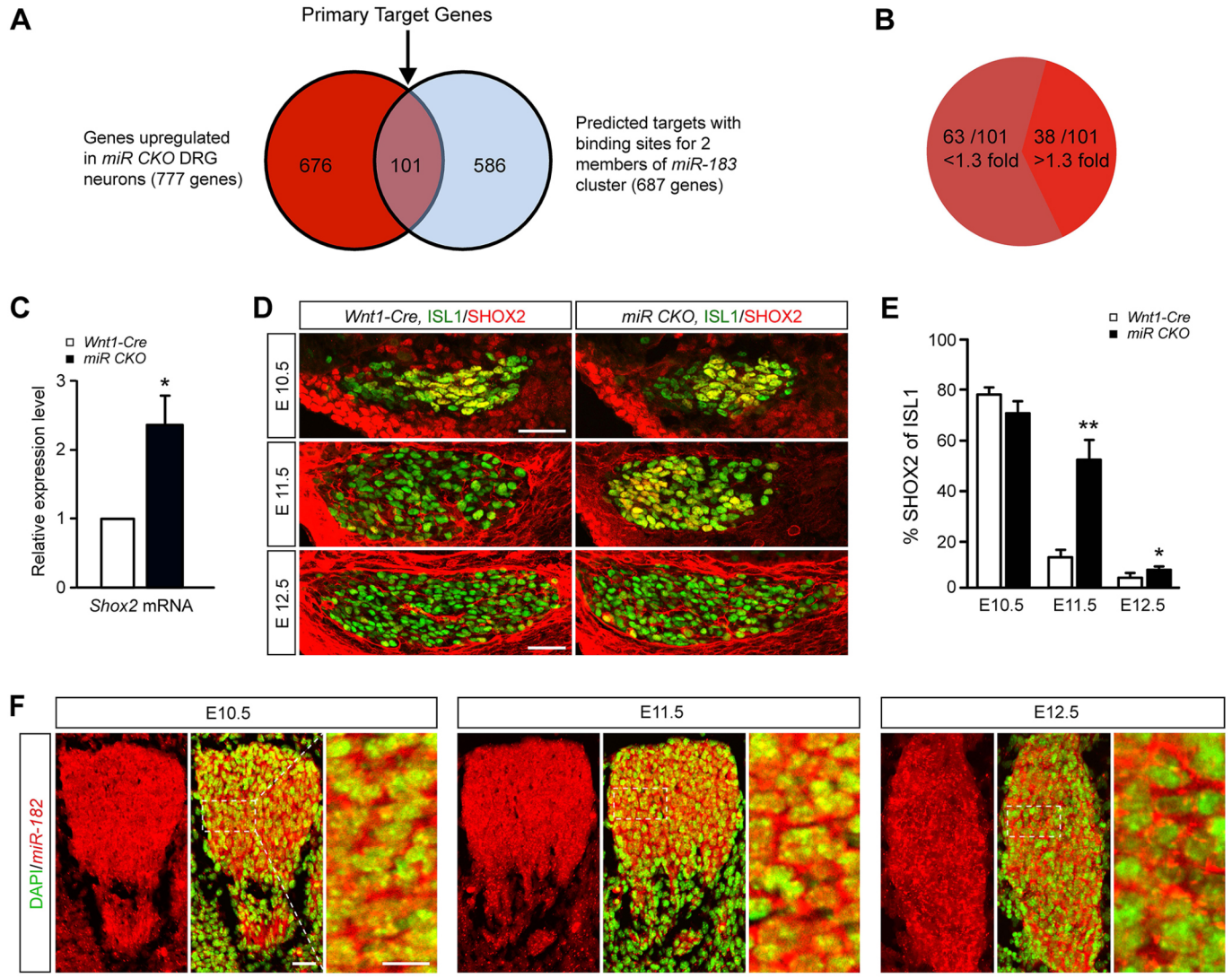

Fig. 2. The miR-183 cluster terminates *Shox2* expression in DRG neurons. (A) Venn diagram shows the significantly upregulated (P<0.05) genes in the E12.5 miR^{CKO} mice from expression profiling data of DRG neurons (red) and TargetScan-predicted mRNA targets with binding sites for more than one member of the miR-183 cluster [blue, Table S1 (Sheet3)]. The overlapping 101 genes were considered as potential targets of the miR-183 cluster. (B) Thirty-eight out of 101 target genes had greater than 1.3-fold increased mRNA expression and the remaining displayed less than 1.3-fold increased expression in miR^{CKO} mice. (C) An increase of 2.3-fold in *Shox2* mRNA levels in the E12.5 miR^{CKO} mice was confirmed by real-time PCR. n=3, data are mean±s.e.m. analyzed by t-test, *P<0.05. (D) SHOX2 is present in most E10.5 DRG neurons and is rapidly lost in most neurons at E11.5 in control mice but failed to be lost in miR^{CKO} mice. (E) Quantification revealed that at E11.5 and E12.5, miR^{CKO} mice had more SHOX2 immunoreactive cells in the DRG than did *Wnt1-Cre* controls, n=4, *P<0.05, **P<0.01 by t-test. (F) *In situ* hybridization for *miR-182* at E10.5, E11.5 and E12.5 revealed that it is ubiquitously expressed in DRG neurons (DAPI, green). Scale bars: 50 µm.

neurons at E10.5, rapidly reduced at E11.5 and barely detected by E12.5 (Fig. 2D,E). $TRKB^+$ and $TRKC^+$ neurons segregate between E11.5 and E12.5 in the lumbar DRG (Kramer et al., 2006); therefore, SHOX2 repression precedes the diversification of these neuron types. SHOX2 extinction between E10.5 and E11.5 failed in miR^{CKO} mice; however, by E12.5 SHOX2 was downregulated similar to control mice (Fig. 2D,E). The finding that *miR-182* was expressed in all DRG neurons throughout this developmental time window (Fig. 2F) indicates that this microRNA cluster works through determining the timing of extinction of SHOX2 rather than establishing selective expression in some but not other cells.

Extension of SHOX2 expression in $TRKC^+$ neurons in the miR^{CKO} mice results in increased numbers of $TRKB^+$ neurons

Our results show that the miR-183 cluster rapidly extinguishes SHOX2 expression at E11.5 in most neurons of the DRG. SHOX2 drives TRKB expression, and in the *Shox2* knockout mice there is a fate switch from $TRKB^+$ neurons to $TRKC^+$ LTMR neurons during this stage of development (Abdo et al., 2011; Scott et al., 2011). This raises the possibility that the miR-183 cluster could determine the proportion of $TRKB^+$ and $TRKC^+$ neurons generated during development by repression of *Shox2* expression. To obtain further insights into the development of LTMRs, we examined DRG at E10.5, prior to SHOX2 repression in most neurons. At this stage, TRKB and TRKC are largely co-expressed in DRG progenitors, which a few days later diversify into $TRKB^+$ LTMRs and $TRKC^+$ neurons, as previously reported (Kramer et al., 2006). Triple immunostaining for SHOX2, TRKC and TRKB showed that, at E10.5 among $TRKC^+$ neurons, virtually all also contained SHOX2 and, among these, 24±3% also co-stained for TRKB. Furthermore, among $TRKB^+$ neurons, all were also $TRKC^+$ and $SHOX2^+$ (Fig. 3A). Thus, SHOX2 is expressed promiscuously both in all

Development (2018) 145, dev165613. doi:10.1242/dev.165613

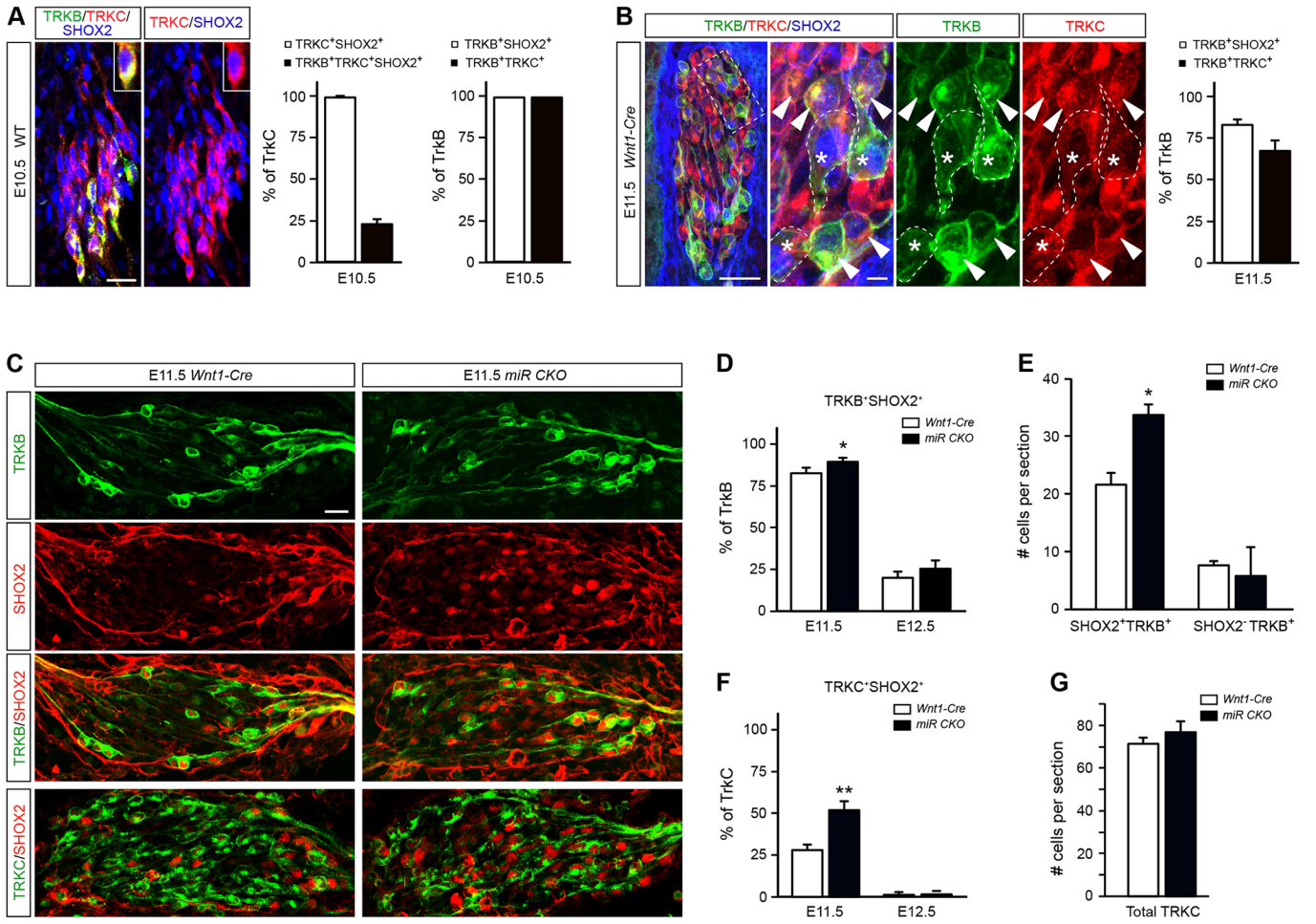

Fig. 3. SHOX2 expression fails to be extinguished in developing sensory neurons of *miR^{CKO}* mice. (A) Immunostaining in wild-type mice for TRKB, TRKC and SHOX2 in E10.5 DRG and quantification to reveal the relation of SHOX2 expression to expression of TRKB and TRKC (n=4). Scale bar: 50 µm. (B) Immunostaining in control *Wnt1-Cre* mice for TRKB, TRKC and SHOX2 in E11.5 DRG, and quantification to reveal the relationship of SHOX2 expression to expression of TRKB and TRKC. Many SHOX2$^+$/TRKB$^+$ neurons lost membrane TRKC$^+$ staining, indicating its downregulation (asterisks), whereas neurons with membrane TRKC staining rarely contained SHOX2 (arrowheads). Quantification is of all positive cells (n=4). Scale bars: 50 µm; 10 µm in the magnified images. (C) Double immunostaining for TRKB/SHOX2 or TRKC/SHOX2 on DRG sections of *Wnt1-Cre* and the *miR^{CKO}* mice. Scale bar: 50 µm. (D) Quantification of the percentage of TRKB$^+$/SHOX2$^+$ neurons to all TRKB neurons in the DRG of E11.5 *Wnt1-Cre* control mice and *miR^{CKO}* mice (n=4), *P<0.05 by Student's t-test. (E) Quantification of the number of SHOX2$^+$/TRKB$^+$ and SHOX2$^-$/TRKB$^+$ neurons revealed an increased number of SHOX2$^+$/TRKB$^+$ DRG neurons in *miR^{CKO}* compared with *Wnt1-Cre* control mice at E11.5 (n=4), *P<0.05 by Student's t-test. (F) Quantification of the percentage of TRKC$^+$/SHOX2$^+$ neurons to all TRKC neurons in the DRG of E11.5 *Wnt1-Cre* control mice and *miR^{CKO}* mice (n=4), **P<0.01 by Student's t-test. (G) Quantification of the number of TRKC$^+$ neurons in DRG of *Wnt1-Cre* control mice and *miR^{CKO}* mice (n=4).

neurons expressing only TRKC and in all neurons expressing TRKB, and these always co-express TRKC at E10.5. This indicates that expression of TRKB is initiated in some of the TRKC$^+$/SHOX2$^+$ neurons. In the E11.5 control *Wnt1-Cre* mouse, TRKB and TRKC remained largely co-expressed, although some neurons started to lose membrane presence of TRKC, which is indicative of its downregulation [consistent with previous results (Kramer et al., 2006)], and SHOX2 was expressed in the majority of the TRKB$^+$ neurons (Fig. 3B).

We next analyzed control mice (*Wnt1-Cre*) and *miR^{CKO}* mice to determine how SHOX2 is expressed between E11.5 and E12.5 when TRKB$^+$/TRKC$^+$ neurons segregate into TRKB$^+$ and TRKC$^+$ neurons (Kramer et al., 2006), which defines the generation of different kinds of LTMRs (Abdo et al., 2011; Bourane et al., 2009; Scott et al., 2011). Immunohistochemical staining indicated the presence of more SHOX2$^+$ neurons and increased numbers of both TRKB$^+$/SHOX2$^+$ and TRKC$^+$/SHOX2$^+$ neurons at E11.5 (Fig. 3C). Quantification revealed in control (*Wnt1-Cre*) mice that SHOX2 expression among TRKB$^+$ neurons was reduced from 84±2% of all TRKB$^+$ neurons at E11.5 to 20±3% at E12.5. In contrast to maintained SHOX2 expression in some TRKB$^+$ neurons at E12.5, it was repressed in nearly all TRKC$^+$ neurons (Fig. 3D,F). Thus, SHOX2 segregates in TRKB- but not TRKC-expressing neurons. In *miR^{CKO}* mice, an increased percentage of TRKB$^+$ neurons contained SHOX2 when compared with control mice at E11.5, but similar to control mice, only about a quarter of the TRKB$^+$ neurons contained SHOX2 at E12.5 (Fig. 3D). Because SHOX2 drives differentiation of the TRKB$^+$ LTMR fate, the shifted temporal repression of SHOX2 predicts that the *miR^{CKO}* mice display an overall increased number of TRKB$^+$ neurons at E11.5. Quantification of the E11.5 DRG revealed that the *miR^{CKO}* mice had more TRKB$^+$/SHOX2$^+$ double-positive neurons than control (*Wnt1-Cre*) mice, whereas there was no change in the number of TRKB$^+$/SHOX2$^-$ neurons (Fig. 3E). This finding is in line with the failure of *Shox2* repression to maintain TRKB expression in neurons that normally should have extinguished TRKB (e.g. TRKC$^+$ neurons). Consistently, the

Development (2018) 145, dev165613. doi:10.1242/dev.165613

percentage of TRKC$^+$ neurons containing SHOX2$^+$ was increased in the *miR^{CKO}* mice when compared with control *Wnt1-Cre* mice, with more than half of all TRKC$^+$ neurons expressing SHOX2 at E11.5 (Fig. 3F) while the total number of TRKC$^+$ neurons was unchanged (Fig. 3G). This shows that when the miR-183 cluster is absent, SHOX2 is maintained in TRKC$^+$ neurons that normally should have lost SHOX2 by E11.5. We therefore conclude that the miR-183 cluster is crucial for a timely extinction of SHOX2 expression at E11.5 when LTMR neurons diversify into distinct types.

Expression of the miR-183 cluster and SHOX2 in the developing human DRG

Since the mature sequences of *miR-183*, *miR-96* and *miR-182* and their binding sites on *Shox2* 3′UTR are highly conserved among vertebrates, from lizard to human (Fig. S2 and data not shown), we next investigated whether the miR-183 cluster, TRKB, TRKC and SHOX2 are expressed in a similar way in the developing human as in rodents. Immunostaining on DRG sections from human embryos at post-conception times 6, 7, 8.5 and 11 weeks showed that TRKB, TRKC and SHOX2 are expressed in many neurons at 6 weeks with reduced number of neurons as development progresses (Fig. 4A-O). TRKB and TRKC were sometimes co-localized in 6- and 7-week-old embryos (asterisk), whereas in 8.5-week-old embryos TRKB and TRKC neurons were largely segregated. This segregation was accompanied by a decline of SHOX2 in TRKC$^+$ neurons from 7-8.5 weeks (Fig. 4F-O, arrows) and at 8.5 weeks, most of TRKC neurons had downregulated SHOX2 (Fig. 4K-O). In contrast, TRKB was also retained in SHOX2$^+$ neurons at later embryonic

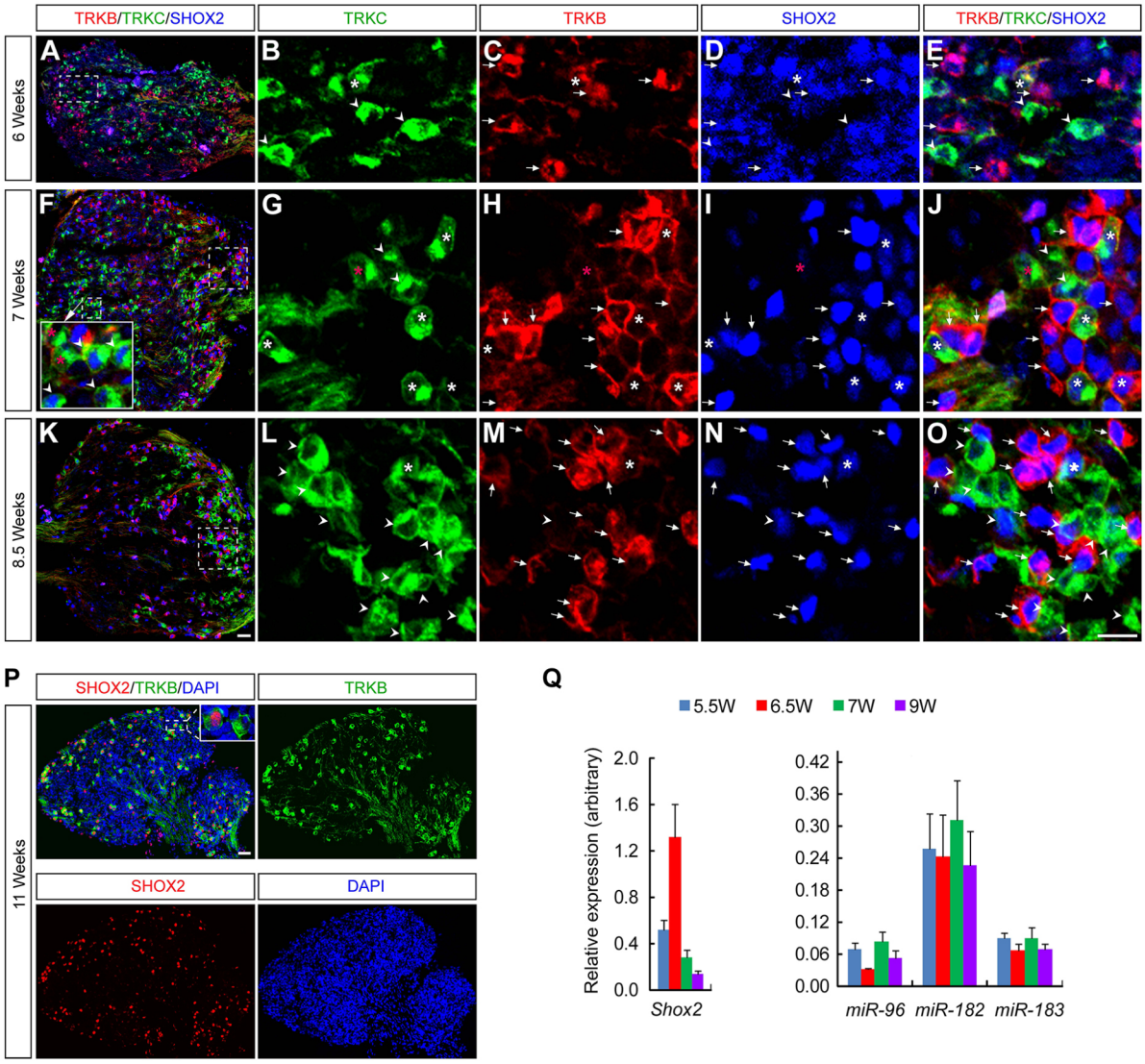

Fig. 4. Expression of the miR-183 cluster and SHOX2 in the developing human DRG. (A-O) Expression of SHOX2 overlapped with TRKB and/or TRKC expression in week 6 and week 7 DRG but very rarely co-exists with TRKC at week 8.5. Triple immunostaining for TRKB (red), TRKC (green) and SHOX2 (blue) on a DRG section of 6- to 8.5-week-old human embryos shows that SHOX2 was weakly expressed in DRG and that some TRKB neurons co-express TRKC at week 6 (B-E are enlargements of the area outlined in A). SHOX2 expression was present in TRKB$^+$ and/or TRKC$^+$ neurons at week 7 (G-J are enlargements of the area outlined in F); however, at 8.5 weeks, SHOX2$^+$ cells were maintained in TRKB$^+$ neurons while most of the TRKC$^+$ neurons lost SHOX2 (L-O are enlargements of the area outlined in K). Arrowheads point to TRKC$^+$ neurons; arrows point to TRKB$^+$ neurons; white asterisks mark TRKB$^+$/TRKC$^+$/SHOX2$^+$ neurons, red asterisks mark TRKC$^+$ neurons expressing lower TRKB and SHOX2. Scale bar: 50 µm. (P) In the 11-week-old human embryo, SHOX2 is extinguished in all but TRKB$^+$ neurons. Scale bar: 50 µm. (Q) Detection of *Shox2* and *miR-183-96-182* expression levels in DRG from 5.5- to 9-week-old human embryos by qPCR. The expression levels of *Shox2* and *miR-183-96-182* were normalized to internal controls 18S RNA and U6B, respectively (data are mean±s.e.m.value of three technical repeats).

Development (2018) 145, dev165613. doi:10.1242/dev.165613

stages (Fig. 4K-O, arrowheads). In 11-week-old embryos, SHOX2 was mostly expressed in TRKB$^+$ neurons (Fig. 4P); however, a few TRKB$^+$ cells were SHOX2$^-$ (inset in Fig. 4P). Expression of *Shox2* mRNA was also confirmed by reverse transcription PCR (RT-PCR) (Fig. 4Q). Together, these data show that expression of TRKB, TRKC and SHOX2 are similarly regulated in human and in mouse. *In situ* hybridization for the miR-183 cluster suggested that all three miRNAs were expressed in human embryonic DRG from 6-8.5 weeks (Fig. S3). Quantitative RT-PCR confirmed expression of the miR-183 cluster, with *miR-182* expressed at the highest level (Fig. 4Q). *miR-96*, which has a higher affinity for the human *Shox2* 3′UTR among the three miRNAs (see Fig. S2), showed the greatest regulation. *miR-96* was first downregulated to about 50% from week 5.5 to week 6, coinciding with elevated levels of *Shox2*. *miR-96* was thereafter substantially increased at week 7, to levels slightly higher than at week 5.5 (Fig. 4Q). Our results demonstrate the similar development of TRKB$^+$ and TRKC$^+$ neurons and miR-183 cluster expression in the embryonic human as in mouse DRG.

The miR-183 cluster determines the adult proportion of Aδ LTMRs and Aβ SA-LTMRs

Our previous results show that miR-183 cluster participates in the diversification of TRKC$^+$/RUNX3$^-$ LTMR but not TRKC$^+$/RUNX3$^+$ proprioceptors (Fig. 1G). Excluding proprioceptors, the only LTMRs expressing TRKC in the adult are Aβ SA-LTMRs (Usoskin et al., 2015). We therefore concluded that miR-183 cluster-dependent repression of TRKB participates in generating the TRKC$^+$ Aβ SA-LTMRs. However, it remained unclear whether the increase of TRKB$^+$ neurons occurred in Aδ LTMRs and/or Aβ RA-LTMRs, because both types express TRKB (Usoskin et al., 2015). To examine whether loss of the miR-183 cluster results in persistent changes of the proportion of the different LTMRs and, if so, which TRKB$^+$ LTMRs type(s) are involved, we collected and analyzed adult DRG from control (*Wnt1-Cre*) and *miR^{CKO}* mice. Quantifying the total number of neurons revealed no differences between the genotypes (Fig. 5A) and, consistent with analyses at P0, the percentage of all neurons expressing TRKC$^+$ was reduced (Fig. 5B). Aβ RA-LTMRs and Aδ LTMRs are molecularly different and can be distinguished by expression of the calcium-binding proteins CALB1 (calbindin) in the former and NECAB2 in the latter. Quantification revealed no changes in the percentage of all neurons expressing TRKB$^+$/CALB1$^+$, whereas the percentage of TRKB$^+$/NECAB2$^+$ neurons was significantly increased (Fig. 5C-E). Thus, this suggests that miR-183 cluster is involved in diversification of a TRKB$^+$/TRKC$^+$ progenitor that segregates into the TrkB^{high}/NECAB2 Aδ LTMRs and TRKC$^+$/RUNX3$^-$ Aβ SA-LTMRs.

The miR-183 cluster targets *Shox2* and efficiently extinguishes its expression in the DRG

To determine whether *Shox2* is a direct target of miR-183 cluster, we cloned the mouse *Shox2* 3′ untranslated region (UTR), which contains the two conserved binding sites for the miR-183 cluster, into a luciferase reporter vector (sensor) and co-transfected this vector together with a *miR-183-96* overexpression vector into HEK-293 cells (Fig. S4). Overexpression of *miR-183-96* repressed luciferase expression from the *Shox2* 3′UTR sensor vector by 58% and this repression was abolished when the conserved seed sequences of *miR-183-96* binding sites in the sensor vectors were mutated (Fig. 6A,B). As there is only one nucleotide difference between the seed sequence of miR-182 and that of miR-96, we examined whether miR-182 can also target *Shox2* 3′UTR. Co-transfection of a miR-182 overexpression vector repressed the luciferase expression from the *Shox2* 3′UTR sensor vector by 43%, and this repression could be fully rescued by mutating the miR-96-binding site on the sensor vectors (Fig. 6A,B). These results show that miR-183 cluster

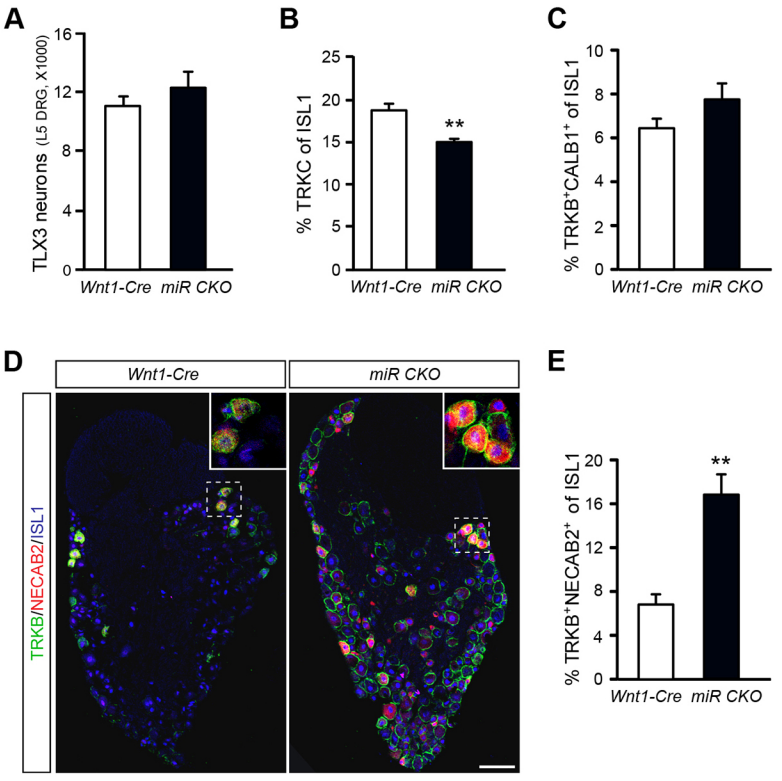

Fig. 5. The miR-183 cluster determines the adult proportion of Aδ LTMRs and Aβ SA-LTMRs but not Aβ RA-LTMRs. (A) Quantification of L5 DRG shows that there was no difference in the total number of neurons between the *miR^{CKO}* mice and age-matched *Wnt1-Cre* control mice, (n=3, P=0.376). (B) The percentage of TRKC$^+$ neurons was decreased in the *miR^{CKO}* mice when compared with control mice (n=3, $^{**}P$<0.01). (C) The percentage of TRKB$^+$/CALB1$^+$ neurons was not significantly changed in the *miR^{CKO}* mice (n=3, P=0.227). (D,E) The percentage of TRKB$^+$/NECAB2$^+$ neurons was increased in the *miR^{CKO}* mice. (D) Triple immunostaining for TRKB (green), NECAB2 (red) and ISL1 (blue) on DRG sections. (E) Quantification in the *miR^{CKO}* mice compared with *Wnt1-Cre* (n=3, $^{**}P$<0.01). Data are mean±s.e.m. and analyzed by t-test. Scale bar: 50 µm.

Development (2018) 145, dev165613. doi:10.1242/dev.165613

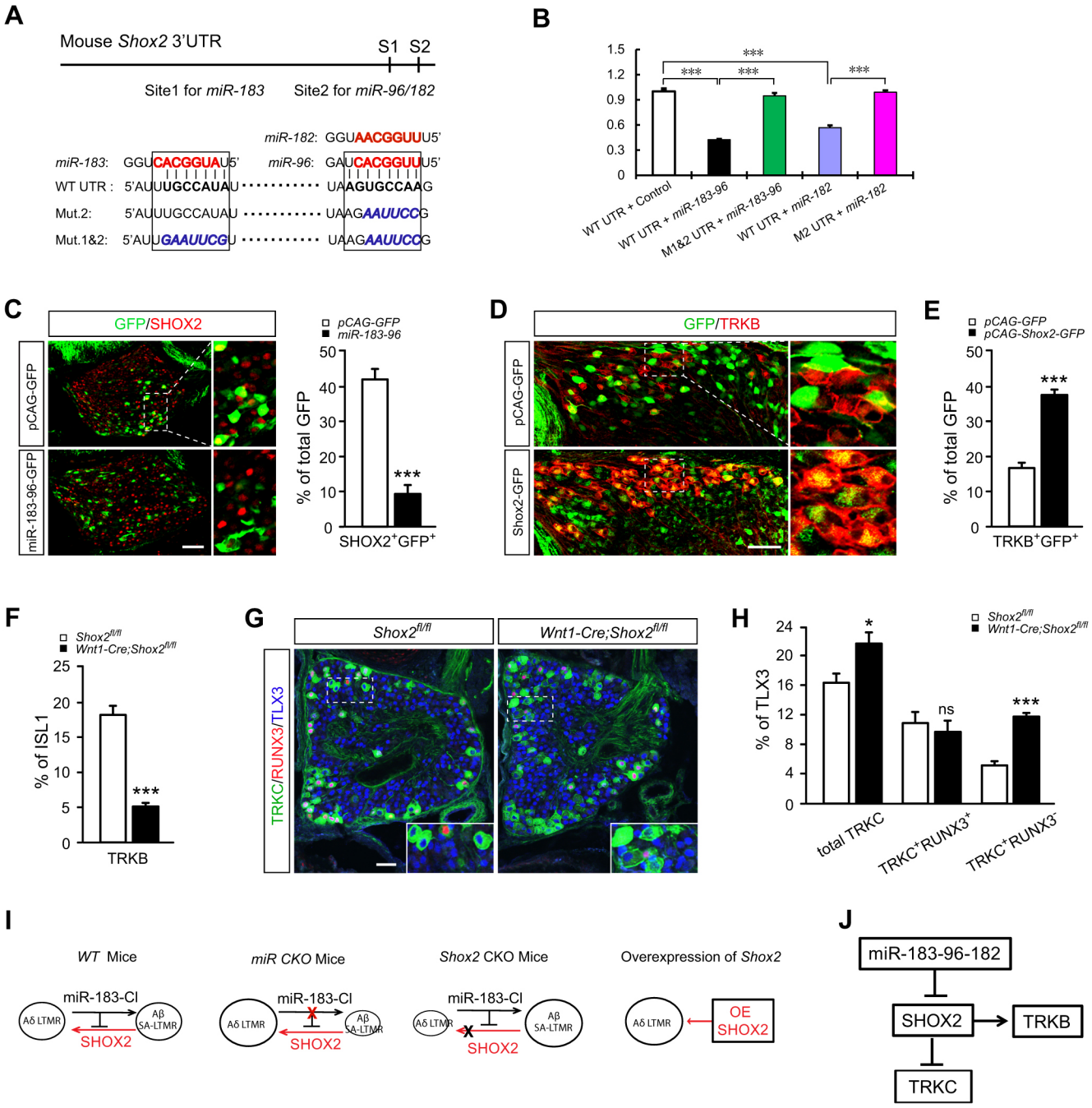

Fig. 6. See next page for legend.

regulates the expression levels of *Shox2* by directly binding to the conserved binding sites located within the 3′UTR. To confirm that the miR-183 cluster can repress *Shox2* expression *in vivo*, we forced expression of *miR-183-96* in chicken DRG by electroporating a *pCAG-miR-183-96-IRES-GFP* vector into the neural tube at the HH13 stage. Embryos were allowed to continue to develop and were analyzed at E7.5, when the neural crest cells have migrated, undergone neurogenesis and coalesced to form the DRG. Quantification showed that the percentage of $GFP^+/SHOX2^+$ cells over total GFP cells was dramatically reduced in the *miR-183-96*-overexpressing group when compared with the control *pCAG-IRES-GFP*-electroporated group (Fig. 6C). These results suggest that the miR-183 cluster can target the *Shox2* mRNA.

The miR-183 cluster diversifies TRKB$^+$ and TRKC$^+$ mechanosensory neurons through regulation of *Shox2*

Based on the strong correlation between upregulation of SHOX2 and the changed proportions of subgroups of DRG neurons in the miR^{CKO} mice, we next investigated whether SHOX2 represents the key target of the miR-183 cluster responsible for the phenotype in the miR^{CKO} mice by using gain-of-function and loss-of-function strategies. Thus, if the miR-183 cluster works through repression of *Shox2*, overexpression of SHOX2 is expected to phenocopy the $miR\text{-}183^{CKO}$ mice and genetic ablation of Shox2 is expected to lead to the reverse phenotype. Overexpression of Shox2 resulted in more than a twofold increase of $TRKB^+$ DRG neurons in chicken embryos (Fig. 6D,E). Crossing *Wnt1-Cre* to $Shox2^{flox/flox}$ mice

Development (2018) 145, dev165613. doi:10.1242/dev.165613

Fig. 6. The miR-183 cluster directly regulates Shox2 to affect the proportions of subgroup neurons in DRG. (A) Schematic illustration of the mouse *Shox2* UTR with two putative binding sites (S1, S2) for the miR-183 cluster. The seed sequence of microRNA is in bold red letters, the binding sequence of the seed sequence is in bold black letters and the mutated binding site sequence is in blue italic letters. The binding site 1 on Shox2 UTR has seven nucleotides that match to miR-183, and binding site 2 has eight and seven nucleotides that match to miR-96 and miR-182, respectively. (B) The miR-183 cluster repressed *Shox2* expression via binding onto its UTR. Co-transfection of *miR-183-96* into HEK293 cells can repress the expression of the *firefly luciferase* gene, which bears a fragment covering S1 and S2 of the Shox2 UTR (black bar) when compared with empty vector-co-transfected control (white bar). This repression was completely abolished when binding sites S1 and S2 were mutated (green bar). miR-182 can also repress the expression of the *firefly luciferase* gene, which bears a fragment covering S1 and S2 of Shox2 UTR (blue bar) when compared with empty vector-co-transfected control (white bar), and the repression was absent when site 2 was mutated (pink bar). ***$P \leq 0.001$. M1&2 stands for mutation on both site 1 and site 2, M2 stands for mutation on site 2. See Fig. S4 for detailed information about the plasmids used. Data are mean±s.d. from four independent experiments repeated in triplicate. (C) Forced expression of *miR-183-96* can repress endogenous SHOX2 expression *in vivo*. Electroporation of the *pCAG-miR-183-96-IRES-GFP* plasmid into neural crest cells of stage HH13 chicken embryo and analysis at E7.5. Immunostaining for SHOX2 (red) and GFP (green) on a DRG section demonstrated that miR-183-96 dramatically repressed endogenous expression of SHOX2 *in vivo* when compared with the *pCAG-IRES-GFP*-electroporated control (n=4 and 3, ***$P \leq 0.001$). (D,E) Overexpression of Shox2 caused an increase of TRKB$^+$ neurons in chicken DRG. Electroporation of *pCAG-Shox2-IRES-GFP* plasmid into neural crest cells of HH13 chicken embryos, which were subsequently harvested at E7.5 and then immunostained for TRKB (red) and GFP (green) on DRG section shows that overexpression of SHOX2 resulted in an increase of TRKB$^+$ neurons when compared with *pCAG-IRES-GFP*-electroporated control (n=4, ***$P \leq 0.0001$). (F) Loss of SHOX2 led to a decrease in the proportion of TRKB$^+$ neurons in the *Wnt1-Cre; Shox2$^{fl/fl}$* mice when compared with *Shox2$^{fl/fl}$* controls (n=3 and 4, ***P<0.001). (G,H) Immunostaining for TRKC (green), RUNX3 (red) and TLX3 (blue) shows that the proportions of TRKC$^+$ (n=3, *P<0.05) and of TRKC$^+$/RUNX3$^-$ (n=3, ***$P \leq 0.001$) neurons to TLX3 neurons in the P0 *Wnt1-Cre; Shox2$^{fl/fl}$* mice were increased, but not TRKC$^+$/RUNX3$^+$ (n=3, P=0.6). (I) Summary of phenotypes observed in the different animal experiments. Aδ LTMR (TRKB$^+$/NECAB2$^+$) and Aβ SA-LTMRs (TRKC$^+$/RUNX3$^-$) refer to the lineage of these types of LTMRs based on marker expression during development. miR-183-CI, miR-183 cluster; OE, overexpression; *miR^{CKO}* mice, *Wnt1-Cre; miR-183-96-182$^{flox/flox}$*; *Shox2* CKO mice, *Wnt1-Cre; Shox2$^{flox/flox}$*. (J) The gene-regulatory network proposed to regulate Aδ LTMR and Aβ SA-LTMRs. Except for B, all data are mean±s.e.m. All data were analyzed by t-test. ns, not significant. Scale bars: 50 µm.

(Abdo et al., 2011) to generate *Wnt1-Cre;Shox2$^{flox/flox}$* mice that have a loss of function of *Shox2* in the DRG revealed a marked reduction of TRKB$^+$ DRG neurons and increased number of TRKC$^+$ DRG neurons at P0, as previously reported (Abdo et al., 2011; Scott et al., 2011) (Fig. 6F-H). Moreover, we found that the TRKC$^+$/RUNX3$^-$ but not TRKC$^+$/RUNX3$^+$ neuron types were increased in the *Wnt1-Cre;Shox2$^{flox/flox}$* mice when compared with the *Shox2$^{flox/flox}$* control mice (Fig. 6G,H). Altogether (see Fig. 6I), our results suggest that the miR-183 cluster works through regulation of *Shox2* in a gene-regulatory network (Fig. 6J), which determines the population sizes of Aδ LTMRs and Aβ SA-LTMRs generated during development.

DISCUSSION

This study represents, to our knowledge, the first molecular identification and characterization of a miRNA that determines the timing of expression of fate-inducing transcription factors in primary sensory neurons. We show that the miR-183 cluster terminates genesis of Aδ LTMRs neurons in favor of Aβ SA-LTMR neurons during development through extinction of *Shox2* expression.

Expression of neurotrophic factor receptors confers ligand sensitivity. Neurotrophic factor signaling plays crucial roles during development for neuron survival, axon growth, peripheral target innervation, patterns of terminations in the spinal cord as well as differentiation into specialized and modality-specific sensors (Lallemend and Ernfors, 2012; Marmigère and Ernfors, 2007). Consequently, expression of growth factor receptors is one of the first distinguished features during cell type diversification in the DRG. However, distinct transcription factor programs are involved in this process, and often interact with growth factor receptor signaling. RUNX3 is crucial for the specification of TRKC-expressing proprioceptive sensory neurons (Levanon et al., 2002) where both BRN3A and RUNX3 are important for repression of TRKB to generate RUNX3$^+$/TRKC$^+$ proprioceptive neurons (Dykes et al., 2010; Kramer et al., 2006). Whereas RUNX3 suppresses *Shox2* expression, SHOX2 is unable to suppress *Runx3* (Abdo et al., 2011). Therefore, initiation of *Runx3* seems to be contributing both by suppressing alternative fates and by initiating the proprioceptive neuron fate. Because of this, neither *Shox2* nor the miR-183 cluster are expected to affect proprioceptive neuron development. This agrees with our results, revealing no effect on TRKC$^+$/RUNX3$^+$ neurons in both the *miR^{CKO}* mice and the *Shox2* CKO mice at P0. Consequently, these findings predict that miR-183 specifically affects development of LTMR neurons involved in touch.

Some neurons acquire RET expression already at E10.5 in the mouse (Molliver et al., 1997), thus coinciding with segregation of other types of LTMRs (e.g. TRKB$^+$ and TRKC$^+$/RUNX3$^-$ neurons). These neurons depend on RET signaling for the specification of RA-LTMRs (Bourane et al., 2009; Honma et al., 2010; Lecoin et al., 2010; Luo et al., 2009). We found no change in total RET$^+$ neurons nor in myelinated NFH$^+$/RET$^+$ neurons at P0. Therefore, our findings predict that miR-183 primarily affects LTMRs rather than early RET$^+$ neurons, which differentiate into Aβ RA-LTMRs. Thus, it seems that RET$^+$ RA-LTMRs and TRKC$^+$/RUNX3$^+$ proprioceptors rely on mechanisms that are independent of the miR-183 cluster.

Consistent with distinct paths for diversification, TRKB$^+$ Aδ LTMRs and TRKC$^+$ Aβ SA-LTMRs seem to emerge from hybrid TRKB$^+$/TRKC$^+$ neurons through extinction of TRKB (Kramer et al., 2006). SHOX2 has been shown to be necessary for proper diversification of TRKB$^+$ neurons, and in its absence, TRKB$^+$ neurons decrease by 60%, whereas TRKC$^+$ neurons increase (Abdo et al., 2011; Scott et al., 2011). In this study, we find that this increase of TRKC$^+$ neurons occurs among TRKC$^+$/RUNX3$^-$ neurons differentiating into LTMRs. SHOX2 therefore participates specifically in the split between neurons that differentiate into Aδ LTMRs and Aβ SA-LTMRs. In this process, the miR-183 cluster determines the timing of *Shox2* extinction, rather than the selective expression in particular cells between E10.5 and E11.5.

Given the fact that all subtypes of sensory neurons in the DRG come from the same progenitor pool derived from trunk neural crest cells, the inversely proportional changes between two related neuron types indicate a shared genetic pathway fating one type and repressing the other. This conclusion is generalized, as numbers do not always add up perfectly. For example, at P0, the percentage increase of TRKB$^+$ neurons is less than the increase of TRKC$^+$ neurons. Thus, this suggests cell fate changes or loss of cells not recorded in this study. Nevertheless, *Shox2* is a direct target for the miR-183 cluster, and the de-repression of *Shox2* in *miR-183^{CKO}* mice appears to be the main mechanism causing the phenotype. Consistent with this, in the *Shox2* CKO mice, the number of TRKB$^+$ neurons decreases and the number of TRKC$^+$ neurons increases, whereas overexpression of

Development (2018) 145, dev165613. doi:10.1242/dev.165613

Shox2 increases TRKB$^+$ neurons; however, in the *miR-183*^{CKO} mice, the number of TRKB$^+$ neurons increases and the number of TRKC$^+$ neurons decreases. Furthermore, the major phenotype of *miR-183*^{CKO} mice and *Shox2* CKO mice encompasses these neuron types, which differentiate into Aδ LTMRs and Aβ LTMRs.

Pre-mi-RNAs are processed to become mature miRNAs by the ribonuclease Dicer (Bernstein et al., 2001; Zhang et al., 2004). Although system-wide deletion of *Dicer* leads to early embryonic lethality (Bernstein et al., 2003), conditional deletion restricted to the peripheral nervous system reveals its indispensable role for cell survival, development and plasticity in the nervous system (Fiorenza and Barco, 2016). In the DRG, loss of *Dicer* results in abnormal development with marked loss of sensory neurons and a failure to produce axonal projections (Zehir et al., 2010). The miR-183 cluster is contained within an −4 kb genomic sequence, is produced as a polycistronic pri-miR transcript (Dambal et al., 2015) and has related seed sequences (Karali et al., 2007; Ryan et al., 2006; Xu et al., 2007). *miR-183* is downregulated in animal models for neuropathic pain and knee joint osteoarthritis (Li et al., 2013; Lin et al., 2014), and, consistently, forced *miR-183* expression by intrathecal injections of lentiviruses attenuate spinal nerve ligation-induced mechanical allodynia (Lin et al., 2014). Furthermore, loss of miR-183 cluster function in the adult results in increased basal mechanical sensitivity and mechanical allodynia (Peng et al., 2017). Interestingly, the increased allodynia during nerve damage involves TRKB$^+$ Aδ LTMRs (Peng et al., 2017). However, this effect of miR-183 cluster-deficiency is caused by increased sensitization/excitability due to the loss of a continuous suppression of auxiliary voltage-gated calcium channel subunit genes (*Cacna2d1* and *Cacna2d2*) in adult mice. Thus, although the miR-183 cluster targets *Shox2* during development that affects cell-type specification, *Cacna2d1* and *Cacna2d2* are targeted in adult, which affects mechanical sensitivity. This miRNA cluster therefore serves different functions in sensory neurons during development when compared with the adult.

Given that the miR-183 cluster and many of its target genes are highly conserved in mammals, it is believed that the miR-183 cluster could play similar roles in human as in mouse. This prediction is enforced by the discovery that a point mutation in miR-96 causes progressive hearing loss in both mouse and human (Lewis et al., 2009; Mencía et al., 2009; Soldà et al., 2012). Our data show that the miR-183 cluster is also highly expressed in the developing DRG of humans along with the direct target gene *Shox2*. These data indicate that the miR-183 cluster play similar roles in the developing human DRG as it does in the mouse.

MATERIALS AND METHODS

Mutant mice

miR-183-96-182$^{flox/+}$ mice (Peng et al., 2017) were crossed with *Wnt1-Cre* 129/SvEv mice (Danielian et al., 1998) to obtain *Wnt1-Cre; miR-183-96-182*$^{flox/+}$ mice. *Wnt1-Cre; miR-183-96-182*$^{flox/+}$ mice were mated to *miR-183-96-182*$^{flox/+}$ mice to obtain *Wnt1-Cre; miR-183-96-182*$^{flox/flox}$ mice and *Wnt1-Cre* control mice. *Wnt1-Cre; Shox2*$^{flox/flox}$ mice were obtained by crossing *Shox2*$^{flox/flox}$ mice (Cobb et al., 2006) with *Wnt1-Cre* mice (Danielian et al., 1998), and the genotyping of the *Shox2* floxed allele and *Wnt1-Cre* was performed as previously described (Abdo et al., 2011). Timed pregnant females were used for collection of embryos; noon of the day of vaginal plug detection was designated as E0.5. All animal work was conducted under ethical permission from the Swedish ethical review panel (norra djurförsöksetiska nämnden).

Human tissue

Human embryonic and fetal tissue was retrieved from elective routine abortions at the Karolinska University Hospital with written consent from the pregnant women, and DRGs were dissected and immersed in 4% PFA for 6 h, further immersed in 20% sucrose overnight after wash in PBS for 5 min, finally embedded in OCT and sectioned at 14 µm. Age (weeks after conception) of the aborted tissue was determined using anatomical landmarks (England, 1990; Yamada and Takakuwa, 2012). Use of human fetal tissue was approved by the Stockholm vetting board on ethics in human research (2007/1477-31, 2011/1101-32 and 2013/564-32).

In situ hybridization and histology

Paraffin sections (8 µm) and cryosections (14 µm) from lumbar mouse and human DRG were processed and hybridizations were performed as described previously (Peng et al., 2012). Digoxigenin (DIG)-labeled LNA probes for *miR-183* (Exiqon) and *miR-182* (Exiqon) were used. Alkaline phosphatase-conjugated anti-digoxigenin antibody (Roche, 1:2000) was used and alkaline phosphatase staining was developed with Fast Red (Roche) and then followed by counterstaining with DAPI or immunostaining for ISL1 [clone 39.4D5; Developmental Studies Hybridoma Bank (DSHB), The University of Iowa, Iowa City, USA, 1:100]. Images were taken using an Olympus FV1000 confocal microscope.

Immunostaining

Immunostaining on 14 µm cryosections from mouse and human lumbar DRG was performed as previously described (Abdo et al., 2011). The following primary antibodies were used: mouse antibodies against ISL1 (DSHB, 1:100), SHOX2 (Santa Cruz, 1:400), NFH (neurofilament, heavy polypeptide) (CloneN52; Sigma Aldrich, 1:500); rabbit antibodies against RUNX3 (gifts from Thomas Jessell, Columbia University Medical Center, NY, USA; 1:300), ISL1 (gifts from Thomas Jessell, 1:250), NFH (Millipore, 1:200), TRKA (Millipore, 1:500), TRKC (Cell Signaling, 1:500), NECAB2 (Proteintech Europe, 1:1000), CALB1 (Millipore, 1:500) and chicken TRKB (a kind gift from Louis F. Reichardt, University of California, USA; 1:2000); goat antibodies against TRKA (R&D systems, 1:500), TRKB (R&D systems, 1:500), TRKC (R&D systems, 1:500), Ret (R&D systems, 1:100) and GFP (Abcam, 1:500); guinea pig antibodies against TLX3 (a kind gift from Carmen Birchmeier, Max Delbruck Center for Molecular Medicine, Germany, 1:10 000). Secondary antibodies were fluorescently labeled (AlexaFluor 405/488/594/647; Molecular Probes and Invitrogen). Fluorescent images were taken with a confocal laser scanning microscope (Olympus FV1000 confocal microscope or Zeiss LSM700) and processed with Adobe Photoshop CS software.

Quantification methods

All markers were counted on DRG sections at either lumbar level 4-6 (*Wnt1-Cre* control and *miR*^{CKO} mice) or brachial level (*Wnt1-Cre; Shox2*$^{flox/flox}$ and *Shox2*$^{flox/flox}$ mice). TRKA$^+$, TRKB$^+$, TRKC$^+$, ISL1$^+$ and SHOX2$^+$ cells were counted on eight position-matched sections from each *Wnt1-Cre* control and *miR*^{CKO} embryo. To analyze the proportion of each marker at the P0 stage, the numbers of TRKA$^+$, TRKB$^+$, TRKC$^+$, RUNX3$^+$, RET$^+$ and NFH$^+$ cells were counted on at least the three biggest sections from three DRG per *Wnt1-Cre* control, *miR*^{CKO}, *Wnt1-Cre; Shox2*$^{flox/flox}$ and *Shox2*$^{flox/flox}$ mouse, then normalized to the number of total neurons (ISL1$^+$ or TLX3$^+$) on the same sections. To get the numbers of total neurons in L5 DRG at P0 (ISL1$^+$) and adult (TLX3$^+$), every ninth serial section through L5 ganglion was counted, then multiplied by eight to get the number of total neurons in L5 DRG. TRKB$^+$, CALB1$^+$, NECAB2$^+$, TRKC$^+$, TRKA$^+$ and NFH$^+$ cells were counted on every ninth serial section through L5 ganglion of *Wnt1-Cre* control and the *miR*^{CKO} adult mice (5-6 months), and the number cells positive for each marker was then normalized to the number of TLX3$^+$ neurons for comparison. All values shown are mean±s.e.m. Statistical significance between groups was assessed by *t*-tests using GraphPad Prism 5. A value of $P<0.05$ was considered significant.

Expression profiling of DRG

Mouse lumbar DRG tissue was dissected from E12.5 three controls (two *Wnt1-Cre* and one wild type) and three *miR*^{CKO} embryos. Total RNA was isolated using Trizol Reagent (Invitrogen) and processed with TruSeq Stranded mRNA Sample Prep Kit (Illumina/USA) according to the manual to obtain the cDNA library. The adapter-ligated libraries were sequenced on the Illumina sequencer according to the manufacturer's instructions.

Development (2018) 145, dev165613. doi:10.1242/dev.165613

Read processing was performed as described previously (Islam et al., 2014), except that the molecule counting by unique molecule identifiers was omitted. Alignments against UCSC mm10 genome were made with bowtie1 version 0.12.9 (Langmead et al., 2009), allowing for up to three mismatches. RPKM values were obtained by dividing each read count by the transcript length in kb and normalizing to a total of 1 million in each sample. Profiling data from mouse DRG (Table S1, sheet 1) were then analyzed using Qlucore Omics Explore, and significantly (P<0.05) upregulated genes (Table S1, sheet 2) in the miR^{CKO} DRG were matched to the targets (Table S1, sheet 3) predicted by TargetScan algorithm. The 38 overlapped genes with upregulation of more than 1.3-fold are listed in Table S1, sheet 4.

Vector constructs

The genomic sequences (shown in Table S1, sheet 5) for *miR-183-96* and *miR-182* were synthesized and cloned into *pCAGIG* vector (Addgene, 11159). Levels of *miR-183*, *miR-96* and *miR-182* expression from the OE vectors *pCAG-miR-183-96-IRES-GFP* and *pCAG-miR-182-IRES-GFP* were quantified by real-time RT-PCR after transfection into HEK-293 cells (Fig. S4). The mouse *Shox2* 3′UTR (Entrez Gene Accession number NM_001302357.1) was amplified from cDNA of E12.5 DRG with the primers indicated in Table S1, sheet 6, and cloned into the *Xba*I site downstream of the Luciferase CDS in the *pGL3* promoter vector (Promega) to obtain the *pGL3-Shox2-3′UTR* vector. Binding site-mutated *Shox2* 3′ UTR sequences were directly synthesized and cloned into *pGL3* promoter vectors. Truncated mouse *Shox2* CDS (position 210-1350, without binding sites for the miR-183 cluster, Entrez Gene Accession number NM_013665.1) was subcloned from pGEMT-Shox2 cDNA plasmid (a gift from J. Cobb, University of Calgary, Canada) into the *pCAGIG* vector to obtain the *pCAG-Shox2-IRES-GFP* OE vector.

Luciferase reporter assays

The miRNA sensor assays were conducted in HEK293 cells co-transfected with 500 ng/well *pGL3-Shox2-3′UTR* sensor vector and 10 ng/well *pRL-SV40* (internal transfection control) along with 1 µg/well *pCAG-miR-183-96-IRES-GFP* vector or 1 µg/well *pCAG-miR-182-IRES-GFP* vector using Lipofectamine 2000 (Invitrogen). The corresponding rescue assays were carried out in HEK293 cells co-transfected with 500 ng/well *pGL3-mut-Shox2-3′UTR* sensor vector with 1 µg/well *pCAG-miR-183-96-IRES-GFP* vector or 1 µg/well *pCAG-miR-182-IRES-GFP* and 10 ng/well *pRL-SV40* vector. Cells were lysed in passive lysis buffer 40 h post-transfection, and Firefly and Renilla Luciferase luminescence was measured in a Victor luminometer (Wallac Sverige) using the Dual-Luciferase Reporter Assay system (Promega) according to the manufacturers' instructions. Firefly luminescence was normalized against Renilla luminescence for each well. Assays were performed in triplicate and data are derived from three independent experiments.

Real-time RT-PCR (qRT-PCR) assays

Total RNA was isolated from mouse DRG, human DRG and HEK-293 cells using Trizol Reagent (Invitrogen) and treated with RNase-free DNase I (Qiagen). Total RNA (0.5-1 µg) was polyadenylated and reverse transcribed using Catch-All miRNA&mRNA RT-PCR Kit (Pengekiphen) according to the manufacturer's instructions. For detection of miRNA expression levels, qRT-PCR assays were conducted using the Catch-All miRNA&mRNA universal PCR primer as a reverse primer and the specific miRNA forward primers listed in Table S1, sheet 6. The amplification conditions were an initial step at 95°C for 10 min, followed by 40 cycles of 15 s at 95°C and 1 min at 60°C. All assays were performed in triplicate and included negative controls. The Ct value was recorded for each reaction, and the expression level of miRNA was calculated relative to *U6B*, a ubiquitously expressed snRNA, and *Shox2* was normalized to either *Gapdh* or *18S RNA*. Data are presented as target gene expression=$2^{-\Delta ct}$.

In ovo electroporation

pCAG-Shox2-IRES-GFP, *pCAG-miR-183-96-IRES-GFP* or backbone vector *pCAGIG* were injected into the neural tube of stage HH13 chicken embryos. Electroporation by five pulses of 40 V/cm was performed using a square wave electroporator (BTX). Embryos were harvested at E7.5 and fixed in 4% PFA/PBS for 6 h at 4°C and sectioned at 14 µm.

Acknowledgements

We thank Mr Thomas Tingström for great help with taking care of all the mice. We also thank Sten Linnarsson's group for providing assistance in RNA sequencing.

Competing interests

The authors declare no competing or financial interests.

Author contributions

Conceptualization: C.P., P.E.; Methodology: C.P., A.F., M.-D.Z., J. Su, M.L., P.L., H.A., E.S.; Software: P.L., J. Sontheimer; Validation: C.P.; Formal analysis: P.L.; Investigation: C.P., A.F., M.-D.Z., J. Su, M.L., H.A.; Resources: H.A., E.S.; Writing - original draft: C.P., P.E.; Writing - review & editing: A.F., M.-D.Z., J. Su, M.L., P.L., J. Sontheimer, E.S.; Visualization: J. Sontheimer; Supervision: P.E.; Project administration: C.P.; Funding acquisition: P.E.

Funding

P.E. is supported by the Medicinska forskningsrådet, the Knut och Alice Wallenbergs Stiftelse (Wallenberg Scholar and Wallenberg project grant), Söderbergs Stiftelse, the European Research Council (PainCells 740491) and the Karolinska Institutet. C.P. is supported by the National Natural Science Foundation of China (31741057). Human tissue retrieval was supported by CIMED.

Data availability

All sequence data are available in GEO under the accession number GSE110714.

Supplementary information

Supplementary information available online at
http://dev.biologists.org/lookup/doi/10.1242/dev.165613.supplemental

References

Abdo, H., Li, L., Lallemend, F., Bachy, I., Xu, X.-J., Rice, F. L. and Ernfors, P. (2011). Dependence on the transcription factor Shox2 for specification of sensory neurons conveying discriminative touch. *Eur. J. Neurosci.* **34**, 1529-1541.

Abraira, V. E. and Ginty, D. D. (2013). The sensory neurons of touch. *Neuron* **79**, 618-639.

Bak, M., Silahtaroglu, A., Moller, M., Christensen, M., Rath, M. F., Skryabin, B., Tommerup, N. and Kauppinen, S. (2008). MicroRNA expression in the adult mouse central nervous system. *RNA* **14**, 432-444.

Bernstein, E., Caudy, A. A., Hammond, S. M. and Hannon, G. J. (2001). Role for a bidentate ribonuclease in the initiation step of RNA interference. *Nature* **409**, 363-366.

Bernstein, E., Kim, S. Y., Carmell, M. A., Murchison, E. P., Alcorn, H., Li, M. Z., Mills, A. A., Elledge, S. J., Anderson, K. V. and Hannon, G. J. (2003). Dicer is essential for mouse development. *Nat. Genet.* **35**, 215-217.

Bourane, S., Garces, A., Venteo, S., Pattyn, A., Hubert, T., Fichard, A., Puech, S., Boukhaddaoui, H., Baudet, C., Takahashi, S. et al. (2009). Low-threshold mechanoreceptor subtypes selectively express MafA and are specified by Ret signaling. *Neuron* **64**, 857-870.

Busskamp, V., Krol, J., Nelidova, D., Daum, J., Szikra, T., Tsuda, B., Jüttner, J., Farrow, K., Scherf, B. G., Alvarez, C. P. P. et al. (2014a). miRNAs 182 and 183 are necessary to maintain adult cone photoreceptor outer segments and visual function. *Neuron* **83**, 586-600.

Busskamp, V., Krol, J., Nelidova, D., Daum, J., Szikra, T., Tsuda, B., Juttner, J., Farrow, K., Scherf, B. G., Alvarez, C. P. P. et al. (2014b). MiRNAs 182 and 183 are necessary to maintain adult cone photoreceptor outer segments and visual function. *Hum. Gene. Ther.* **25**, A23-A24.

Chalfie, M., Horvitz, H. R. and Sulston, J. E. (1981). Mutations that lead to reiterations in the cell lineages of C. elegans. *Cell* **24**, 59-69.

Cobb, J., Dierich, A., Huss-Garcia, Y. and Duboule, D. (2006). A mouse model for human short-stature syndromes identifies Shox2 as an upstream regulator of Runx2 during long-bone development. *Proc. Natl. Acad. Sci. USA* **103**, 4511-4515.

Dambal, S., Shah, M., Mihelich, B. and Nonn, L. (2015). The microRNA-183 cluster: the family that plays together stays together. *Nucleic Acids Res.* **43**, 7173-7188.

Danielian, P. S., Muccino, D., Rowitch, D. H., Michael, S. K. and McMahon, A. P. (1998). Modification of gene activity in mouse embryos in utero by a tamoxifen-inducible form of Cre recombinase. *Curr. Biol.* **8**, 1323-1326.

Dykes, I. M., Lanier, J., Eng, S. R. and Turner, E. E. (2010). Brn3a regulates neuronal subtype specification in the trigeminal ganglion by promoting Runx expression during sensory differentiation. *Neural Dev.* **5**, 3.

England, M. A. (1990). *A Color Atlas of Life Before Birth: Normal Fetal Development*. London: Wolfe Medical Publications.

Fiorenza, A. and Barco, A. (2016). Role of Dicer and the miRNA system in neuronal plasticity and brain function. *Neurobiol. Learn. Mem.* **135**, 3-12.
Gu, C., Li, X., Tan, Q., Wang, Z., Chen, L. and Liu, Y. (2013). MiR-183 family regulates chloride intracellular channel 5 expression in inner ear hair cells. *Toxicol. In vitro* **27**, 486-491.
Honma, Y., Kawano, M., Kohsaka, S. and Ogawa, M. (2010). Axonal projections of mechanoreceptive dorsal root ganglion neurons depend on Ret. *Development* **137**, 2319-2328.
Islam, S., Zeisel, A., Joost, S., La Manno, G., Zajac, P., Kasper, M., Lönnerberg, P. and Linnarsson, S. (2014). Quantitative single-cell RNA-seq with unique molecular identifiers. *Nat. Methods* **11**, 163-166.
Karali, M., Peluso, I., Marigo, V. and Banfi, S. (2007). Identification and characterization of microRNAs expressed in the mouse eye. *Invest. Ophthalmol. Vis. Sci.* **48**, 509-515.
Kramer, I., Sigrist, M., de Nooij, J. C., Taniuchi, I., Jessell, T. M. and Arber, S. (2006). A role for Runx transcription factor signaling in dorsal root ganglion sensory neuron diversification. *Neuron* **49**, 379-393.
Lagos-Quintana, M., Rauhut, R., Meyer, J., Borkhardt, A. and Tuschl, T. (2003). New microRNAs from mouse and human. *RNA* **9**, 175-179.
Lallemend, F. and Ernfors, P. (2012). Molecular interactions underlying the specification of sensory neurons. *Trends Neurosci.* **35**, 373-381.
Langmead, B., Trapnell, C., Pop, M. and Salzberg, S. L. (2009). Ultrafast and memory-efficient alignment of short DNA sequences to the human genome. *Genome Biol.* **10**, R25.
Lecoin, L., Rocques, N., El-Yakoubi, W., Ben Achour, S., Larcher, M., Pouponnot, C. and Eychene, A. (2010). MafA transcription factor identifies the early ret-expressing sensory neurons. *Dev. Neurobiol.* **70**, 485-497.
Lee, R. C., Feinbaum, R. L. and Ambros, V. (1993). The C. elegans heterochronic gene lin-4 encodes small RNAs with antisense complementarity to lin-14. *Cell* **75**, 843-854.
Levanon, D., Bettoun, D., Harris-Cerruti, C., Woolf, E., Negreanu, V., Eilam, R., Bernstein, Y., Goldenberg, D., Xiao, C., Fliegauf, M. et al. (2002). The Runx3 transcription factor regulates development and survival of TrkC dorsal root ganglia neurons. *EMBO J.* **21**, 3454-3463.
Lewis, M. A., Quint, E., Glazier, A. M., Fuchs, H., De Angelis, M. H., Langford, C., van Dongen, S., Abreu-Goodger, C., Piipari, M., Redshaw, N. et al. (2009). An ENU-induced mutation of miR-96 associated with progressive hearing loss in mice. *Nat. Genet.* **41**, 614-618.
Li, X., Kroin, J. S., Kc, R., Gibson, G., Chen, D., Corbett, G. T., Pahan, K., Fayyaz, S., Kim, J.-S., van Wijnen, A. J. et al. (2013). Altered spinal microRNA-146a and the microRNA-183 cluster contribute to osteoarthritic pain in knee joints. *J. Bone Miner. Res.* **28**, 2512-2522.
Lin, C.-R., Chen, K.-H., Yang, C.-H., Huang, H.-W. and Sheen-Chen, S.-M. (2014). Intrathecal miR-183 delivery suppresses mechanical allodynia in mononeuropathic rats. *Eur. J. Neurosci.* **39**, 1682-1689.
Liu, Y. and Ma, Q. (2011). Generation of somatic sensory neuron diversity and implications on sensory coding. *Curr. Opin. Neurobiol.* **21**, 52-60.
Lumayag, S., Haldin, C. E., Corbett, N. J., Wahlin, K. J., Cowan, C., Turturro, S., Larsen, P. E., Kovacs, B., Witmer, P. D., Valle, D. et al. (2013). Inactivation of the microRNA-183/96/182 cluster results in syndromic retinal degeneration. *Proc. Natl. Acad. Sci. USA* **110**, E507-E516.
Luo, W., Enomoto, H., Rice, F. L., Milbrandt, J. and Ginty, D. D. (2009). Molecular identification of rapidly adapting mechanoreceptors and their developmental dependence on ret signaling. *Neuron* **64**, 841-856.
Marmigère, F. and Ernfors, P. (2007). Specification and connectivity of neuronal subtypes in the sensory lineage. *Nat. Rev. Neurosci.* **8**, 114-127.
Mencía, A., Modamio-Høybjør, S., Redshaw, N., Morín, M., Mayo-Merino, F., Olavarrieta, L., Aguirre, L. A., del Castillo, I., Steel, K. P., Dalmay, T. et al. (2009). Mutations in the seed region of human miR-96 are responsible for nonsyndromic progressive hearing loss. *Nat. Genet.* **41**, 609-613.
Molliver, D. C., Wright, D. E., Leitner, M. L., Parsadanian, A. S., Doster, K., Wen, D., Yan, Q. and Snider, W. D. (1997). IB4-binding DRG neurons switch from NGF to GDNF dependence in early postnatal life. *Neuron* **19**, 849-861.
Peng, C., Li, N., Ng, Y.-K., Zhang, J., Meier, F., Theis, F. J., Merkenschlager, M., Chen, W., Wurst, W. and Prakash, N. (2012). A unilateral negative feedback loop between miR-200 microRNAs and Sox2/E2F3 controls neural progenitor cell-cycle exit and differentiation. *J. Neurosci.* **32**, 13292-13308.
Peng, C., Li, L., Zhang, M.-D., Bengtsson Gonzales, C., Parisien, M., Belfer, I., Usoskin, D., Abdo, H., Furlan, A., Häring, M. et al. (2017). miR-183 cluster scales mechanical pain sensitivity by regulating basal and neuropathic pain genes. *Science* **356**, 1168-1171.
Ryan, D. G., Oliveira-Fernandes, M. and Lavker, R. M. (2006). MicroRNAs of the mammalian eye display distinct and overlapping tissue specificity. *Mol. Vis.* **12**, 1175-1184.
Sacheli, R., Nguyen, L., Borgs, L., Vandenbosch, R., Bodson, M., Lefebvre, P. and Malgrange, B. (2009). Expression patterns of miR-96, miR-182 and miR-183 in the developing inner ear. *Gene Expr. Patterns* **9**, 364-370.
Scott, A., Hasegawa, H., Sakurai, K., Yaron, A., Cobb, J. and Wang, F. (2011). Transcription factor short stature homeobox 2 is required for proper development of tropomyosin-related kinase B-expressing mechanosensory neurons. *J. Neurosci.* **31**, 6741-6749.
Soldà, G., Robusto, M., Primignani, P., Castorina, P., Benzoni, E., Cesarani, A., Ambrosetti, U., Asselta, R. and Duga, S. (2012). A novel mutation within the MIR96 gene causes non-syndromic inherited hearing loss in an Italian family by altering pre-miRNA processing. *Hum. Mol. Genet.* **21**, 577-585.
Usoskin, D., Furlan, A., Islam, S., Abdo, H., Lönnerberg, P., Lou, D., Hjerling-Leffler, J., Haeggström, J., Kharchenko, O., Kharchenko, P. V. et al. (2015). Unbiased classification of sensory neuron types by large-scale single-cell RNA sequencing. *Nat. Neurosci.* **18**, 145-153.
Wightman, B., Ha, I. and Ruvkun, G. (1993). Posttranscriptional regulation of the heterochronic gene lin-14 by lin-4 mediates temporal pattern formation in C. elegans. *Cell* **75**, 855-862.
Xu, S., Witmer, P. D., Lumayag, S., Kovacs, B. and Valle, D. (2007). MicroRNA (miRNA) transcriptome of mouse retina and identification of a sensory organ-specific miRNA cluster. *J. Biol. Chem.* **282**, 25053-25066.
Yamada, S. and Takakuwa, T. (2012). Introduction - developmental overview of the human embryo. In *The Human Embryo* (ed. S. Yamada), pp. 3-20. London, England: InTech.
Zehir, A., Hua, L. L., Maska, E. L., Morikawa, Y. and Cserjesi, P. (2010). Dicer is required for survival of differentiating neural crest cells. *Dev. Biol.* **340**, 459-467.
Zhang, H., Kolb, F. A., Jaskiewicz, L., Westhof, E. and Filipowicz, W. (2004). Single processing center models for human Dicer and bacterial RNase III. *Cell* **118**, 57-68.
Zhu, Q., Sun, W., Okano, K., Chen, Y., Zhang, N., Maeda, T. and Palczewski, K. (2011). Sponge transgenic mouse model reveals important roles for the microRNA-183 (miR-183)/96/182 cluster in postmitotic photoreceptors of the retina. *J. Biol. Chem.* **286**, 31749-31760.